Excited States and Intermediate Species of Benzo[*e*]pyrene Photolyzed in Solution and Adsorbed on Surfaces

Silvina Fioressi and Rafael Arce*

Department of Chemistry, University of Puerto Rico, P.O. Box 23346, San Juan, Puerto Rico 00931-3346

Received: October 24, 2002; In Final Form: April 25, 2003

Benzo[*e*]pyrene (BeP) is a widespread polycyclic aromatic hydrocarbon found principally in highly polluted areas. The study of its photochemistry is important because of its possible toxic nature and its potential for phototransformation into biologically active products. We studied the primary photophysical and photochemical degradation processes of BeP, both in solution and adsorbed on silica gel and alumina, acting as models for the atmospheric particulate matter. The radical cation of BeP was characterized as an intermediate species during the photodegradation of BeP in polar solvents and adsorbed on the surfaces. The photoionization process was monophotonic, and once the radical cation was formed, it could react with water or oxygen to yield mainly diones, alcohols, and diols. In alumina, the radical yield was small, in accordance with the low photoreactivity observed on this surface. Two triplet−triplet absorption bands at 350 and 560 nm were observed in the time-resolved spectra of adsorbed BeP and in solution under nitrogen atmosphere. The BeP's triplet state, however, did not play an important role in its photoreaction pathway. The surface's pore size and the coadsorbed water affected the yields and kinetics of the intermediates but not the photodegradation mechanism.

Introduction

There is considerable interest regarding the possible adverse effects on human health by chemical carcinogens encountered in the atmospheric environment. Polycyclic aromatic hydrocarbons (PAHs) were among of the first atmospheric pollutants to be identified as carcinogenic.[1] This class of compounds is ubiquitous in the urban atmosphere and has been the subject of numerous investigations.[2] PAHs can be formed from the incomplete combustion process or by the high-temperature pyrolysis of fossil fuels or, more generally, any organic material.[3] Benzo[*e*]pyrene (BeP) is a PAH present in the atmospheric particulate matter with teratogenic and possibly mutagenic activity. Although the toxicity of BeP has not been clearly established, it is included in the National Oceanic and Atmospheric Administration's (NOAA's) list of PAHs that are recommended for environmental scanning.[4] A mild mutagenicity of BeP has been demonstrated in mice, particularly when combined with other PAHs.[5] In contrast with BeP, a greater number of studies exist on the high BaP toxicity in vitro, in vivo, on animals, and on humans.[6] There are still unanswered questions regarding the large differences in carcinogenic and mutagenic activities of these benzopyrenes. A possible explanation is the lower ionization potential of BaP as compared to BeP and the lower chemical reactivity of BeP to produce oxygenated derivatives in the organisms.

Atmospheric PAHs can undergo thermal and photochemical modification, resulting in products that may have higher or lower toxicity than their precursors. Adsorbed PAHs undergo photodegradation in the presence of oxygen to produce oxidized products such as diones, mono- and dihydrodiols, epoxides, and in some cases carboxylic derivatives.[7] Photooxidation has been shown to proceed mainly through two mechanisms:[8] (a) an electron-transfer reaction from the excited PAH to oxygen to form superoxide and the PAH radical cation (type I); (b) energy transfer from an excited PAH to oxygen to form singlet molecular oxygen (type II).[9] Under laboratory conditions, the photolytic half-lives for particle-bound PAHs are highly dependent on the substrate to which they are adsorbed.[10−15] Generally, PAHs tend to photodegrade more slowly when adsorbed on unactivated alumina than on silica.[10,11] Thermal reactions (or dark reactions) are, however, more frequently observed on alumina surfaces than on silica,[11] perhaps because the acidic and basic properties of the alumina induce, to some extent, the ionization on the adsorbed PAH without irradiation.[12] Due to the limited movement of adsorbed PAH molecules on the time scale of photochemical reactions,[13] the distribution of the PAH on the surface and its interaction with the active sites of the adsorbent determine its photochemistry. Substrates with large surface areas have more active sites, and thus a larger capacity to adsorb PAH molecules. Also, the distribution of active sites on the surface can be related to the material's pore size. Ruetten and Thomas[14] have determined that the density of active sites is higher in the small pores than at the open or flat surface. This could result in a greater mobility of the adsorbed molecules on surfaces of larger pores. It is expected that differences in the distribution and mobility of the adsorbed PAH can affect the lifetimes and yields of excited states and intermediate species formed during the irradiation, and therefore its photochemistry.

The water content of the surface may also affect the photochemistry of adsorbed molecules. Unactivated surfaces may contain water percentages in the range of 1−15%.[12] The water molecules are adsorbed on the active sites of the surface, and thus they compete with the adsorption of the PAHs. In addition, the adsorption of water tends to mask the strong acidic or basic active sites on the surface. Thus, the presence of water may affect the adsorption ability of the surface and therefore the distribution of the adsorbed PAH molecules. It was found that pyrene photodegrades at a slower rate when adsorbed on unactivated silica gel than on an activated surface.[15] Because the photodegradation of adsorbed pyrene is proposed to occur

10.1021/jp027305f CCC: $25.00
Published on Web 07/11/2003

through a type I mechanism, the water adsorbed on the surface could weaken the interactions of the PAH with the surface, making the energy-transfer process less efficient on unactivated silica.

Although BeP is ubiquitous in the environment, and it is frequently used as a tracer for the measurement of contaminated atmospheres,[16] there is a lack of information on its photodegradation mechanism, the resulting photoproducts, and the implications of its transformations in the environment. We have determined that the major photoproducts of BeP adsorbed on silica and alumina are diones, whereas hydroxy derivatives are minor products.[17] In this work, we also report on the intermediate species in the photodegradation of BeP in solution and adsorbed on silica gel and alumina to provide fundamental information on its photoreaction mechanism. The effects of the surface physical and chemical properties on the lifetimes and yields of these intermediate species are also presented.

Materials and Methods

Sample Preparation. BeP (Sigma Chemical Co.) was used as received, and its purity was verified to be >99% by HPLC. The solvents used were HPLC grade (Optima, Fisher Scientific). Nonactivated silica gel of 25, 60, and 150 Å average pore size and alumina type F-20 (Aldrich Chemical Co.) were used as adsorbents. The adsorbed samples were prepared by adding a measured volume of a standard solution of BeP in hexane to a weighed amount of adsorbent to obtain the desirable loading concentration. The solvent was evaporated under a N_2 gas flow with continuous stirring. The effect of coadsorbed water was studied by adding deionized water to the adsorbent before adding the standard solution. The resultant mixture was dried under a N_2 gas flow.

Steady-State Absorption and Fluorescence. The absorption and diffuse reflectance spectra were measured in a double-beam Varian Cary 1E spectrophotometer. The instrument was equipped with an integration sphere to analyze the nontransparent solid samples. The excitation and emission spectra of adsorbed samples and solutions were measured in a 4800 SLM spectrofluorometer. For the powdered nontransparent samples, a 2-mm quartz cell was used, and it was placed in the cell holder slightly deviated from a 45° angle from the incident light and the detector.

Time-Resolved Fluorescence. Fluorescence lifetimes were measured in a Photon Technology International (PTI) LaserStrobe system. In this system, a pulse of a nitrogen laser (337 nm, 1.5 mJ/pulse) is focused on the sample cell of a fluorometer (PTI) by means of an optic fiber. The fluorescence intensity at a selected wavelength is measured as a function of time with a photomultiplier consisting of 10 dynodes, permitting a signal amplification of 10^6-10^7. For the measurement of samples of BeP adsorbed on surfaces, the sample cell was placed in a front face arrangement. The scatter signal was measured for each sample using the same sample but measuring the scattered light at the excitation wavelength of the nitrogen laser (337 nm). The BeP's fluorescence decay, recorded at 398 nm, was fitted to an exponential function to determine the corresponding emission lifetime. Lifetime distribution analysis is generally used to study fluorescence lifetimes in adsorbed samples because it provides additional information on the heterogeneity of the system.[18] We found, however, that by fitting to a single-exponential function, the fluorescence decay of adsorbed BeP as well as that of BeP in solution is described adequately. The comparative method was used for the measurement of the fluorescence quantum yields (Φ_f) in solution with naphthalene and anthracene as references.[19] For the adsorbed samples, the Φ_f values were determined using the method developed by Ruetten and Thomas,[14] which consists of measuring the diffuse reflectance spectra of the sample in the presence and in the absence of oxygen acting as a fluorescence quencher. Because the quencher removes the fluorescence emission of the sample, the difference in reflectance in the presence and in the absence of the quencher measures the amount of fluorescence light emitted by the sample. This emitted fluorescence relative to the absorbed light is the fluorescence quantum yield of the solid sample.

Transient Absorption Measurements. Transient absorption spectra and kinetic traces of samples of BeP were recorded after excitation with 266- and 355-nm lights from a Surelite Nd:YAG (Continuum) laser (1−60 mJ/pulse of 6-ns duration). The signal was collected and analyzed using a Labview program. The intensity of the laser output was measured with a Newport 1835 high-power meter. For the solid samples, since these are opaque, the diffuse reflectance mode was used instead of the transmission mode employed for translucent samples. To measure the transient diffuse reflectance spectra of the adsorbed samples, the cell holder was placed approximately at a 60° angle with respect to the laser beam to avoid the entrance of reflected laser light into the detection system. The analyzing beam was provided by a 450-W Xe (Hg) lamp, focused to impinge on the sample cell at an angle deviated slightly from a 90°. A series of lenses were located after the sample cell to focus the diffusely reflected light into the monochromator slits. Special care was taken not to collect the specular reflected light, because this decreases the sensitivity of the measurements. Data for the diffuse reflectance laser photolysis are reported as $1 - R = (I_0 - I)/I_0$. Others[20] have shown that this function is linear with the amount of transient present for values of $1 - R < 0.1$.

The molar absorption coefficient of the triplet−triplet absorption (ϵ_T) of BeP was measured by the energy-transfer method.[21] Anthracene was chosen as triplet energy acceptor for the determination of the ϵ_T of BeP in nonpolar solvents, because its triplet energy (178 kJ/mol) is much lower that that of BeP (221 kJ/mol).[22] The anthracene triplet−triplet absorption was observed at 420 nm ($\epsilon = 64\,700\ M^{-1}\ cm^{-1}$) and at 402 nm ($\epsilon = 19\,800\ M^{-1}\ cm^{-1}$).[23] The concentration of BeP used was in the range of $(2-4) \times 10^{-6}$ M. These solutions presented ground-state absorption intensities at 266 nm of 0.05−0.1 au. The concentration of anthracene was selected to be 5 times higher than that of BeP to ensure that the energy-transfer process was as complete as possible. Three separate anthracene−BeP solutions in hexane were prepared, and at least two measurements of each solution were made. For the determination of the ϵ_T of BeP in acetonitrile, thioxantone (TX) was selected as triplet donor, because the triplet−triplet absorption of anthracene overlaps with the radical signal of BeP in polar solvents. The triplet−triplet absorbance of TX appears at 620 nm with $\epsilon = 30\,000\ M^{-1}\ cm^{-1}$.[23] The TX was excited at 355 nm at a concentration of 1×10^{-5} M (absorbance of 0.05 at 355 nm), while the BeP concentration was 3×10^{-5} M.

The comparative method was used to calculate the triplet quantum yield (ϕ_T) of BeP in polar and nonpolar solvents using the following equation:[24]

$$\frac{\phi_T^{BeP}\epsilon_T^{BeP}}{A_T^{BeP}} = \frac{\phi_T^{Ref}\epsilon_T^{Ref}}{A_T^{Ref}} \qquad (1)$$

where A_T^{Ref} and A_T^{BeP} are the absorbance intensities of the triplet−triplet signal of the reference and the BeP solutions, respectively. Anthracene,[25] phenanthrene,[26] and benzophenone[27]

were used as references since their ϕ_T and ϵ_T are well characterized. At least two measurements for each solution were made, and the measurements on the BeP solutions were taken immediately after the reference to ensure similar experimental conditions.

Electron Spin Resonance. The ESR spectra were recorded on a Bruker ER-200D spectrometer at 100-kHz magnetic field modulation. The samples were irradiated with a 1000-W Xe (Hg) lamp with a band-pass filter (Corning 7-54) and a water filter placed between the sample and the light source. The powder samples were contained in a quartz ESR cell that was placed inside a dewar with liquid nitrogen to maintain the temperature of the system at 77 K. The microwave power was varied in the range of 2−80 mW to investigate the saturation behavior of some samples. The rest of the samples were analyzed using a microwave power of 10 or 20 mW. The magnetic field was calibrated with α,α′-diphenyl-β-picrylhydrazyl (DPPH) powder as standard ($g = 2.0037$).[28]

Photoproducts Characterization. The photoproducts formed on the surface were extracted with methanol in an ice bath to prevent thermal degradation of some unstable photoproducts, stirred for 2 min, and filtered using a syringe with a Millipore disposable filter disk. Twenty microliters of the resultant solution was injected into a Waters HPLC instrument with a 966 diode array UV−vis detector, a Supelcosil-LC-PAH reverse-phase column (Supelco, 5 μm particle size, 4.6 mm diameter, 25 cm length), and acetonitrile as the mobile phase. The main chromatographic peaks were fraction collected and further analyzed by fluorescence and mass spectrometry (Micromass mass spectrometer model Quattro II) using electrospray ionization.

Results and Discussion

Ground-State and Excited Singlet-State Properties. The absorption spectra of benzo[*e*]pyrene in hexane or in methanol consisted of structured bands in the wavelength range between 200 and 340 nm. These bands correspond to $\pi-\pi^*$ transitions with molar absorption coefficients in the order of 10^4 cm^{-1} M^{-1}. The β bands were observed in the range of 250−300 nm, whereas those occurring between 300 and 340 nm are assigned as the p bands. Both bands presented well-resolved vibronic structure. The α bands appeared between 340 and 370 nm, with molar absorption coefficients of the order of 10^2 M^{-1} cm^{-1}, but were very weak and difficult to observe. The diffuse reflectance spectra of BeP adsorbed on silica or alumina were similar to those observed in polar and nonpolar solvents, except for the absence of the β bands at wavelengths smaller than 250 nm due to the strong absorption of the inorganic oxides in this spectral region. Although the bands were broader compared to those observed for BeP in solution, displacement of the absorption maxima or changes in the relative intensities of the bands were not observed. The band broadening was mainly due to the overlap of the rotational and vibrational states of BeP in the adsorbed state. The similarity of the spectra observed for BeP adsorbed on the surface and in solution suggested that no strong electronic interactions between the PAH and the surfaces need to be considered under our experimental conditions.

The fluorescence emission spectra of BeP in methanol presented five bands in the range of 350−450 nm, whereas in hexane only three bands were observed (Figure 1). These differences can be explained in terms of the Ham effect.[29] Because of perturbation in the vibronic coupling due to solute−solvent interactions, the intensity ratio of band I to III was strongly dependent on the solvent polarity. The band most sensitive to solvent polarity was the first band, which corresponds to the 0−0 transition. For instance, in hexane this band was almost missing and appeared as a shoulder. As a rule, the intensity ratio of I/III changed from 0.64 in methanol to 0.36 in hexane, suggesting that BeP can be used as a microenvironment polarity probe.[30] Adsorbed BeP showed absorption and emission spectra similar to those in methanol and acetonitrile. The intensity ratio I/III of BeP adsorbed on silica was 0.72 and on alumina was 0.60, indicating that the PAH on the surface experiences a polar microenvironment. Because the adsorption sites on alumina and silica surfaces are hydroxyl and silanol groups, it is not surprising that this PAH exhibited a spectral behavior similar to that found for these molecules in polar solvents. These results are in agreement with similar behaviors observed for other adsorbed PAHs.[31]

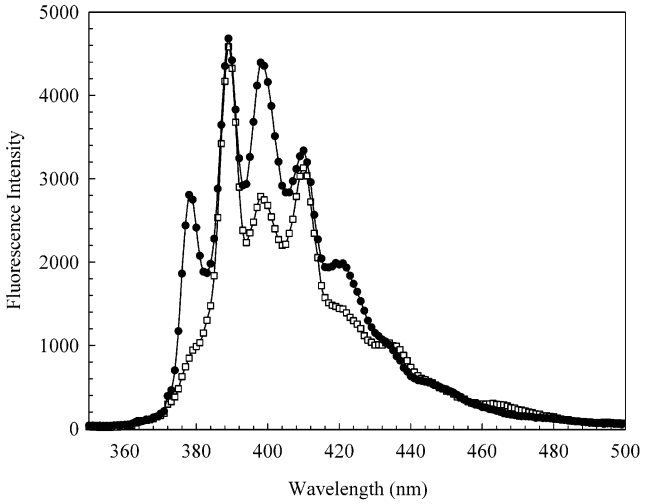

Figure 1. Fluorescence emission spectra of BeP, 4.3×10^{-6} M, in hexane (□) and in methanol (●). The excitation wavelength was 330 nm.

TABLE 1: Fluorescence Quantum Yields and Lifetimes of BeP Adsorbed on Silica Gel[a]

adsorbent	surface loading (mol/g)	Φ_f	τ_f (ns)
silica gel, 25 Å	1.3×10^{-7}	0.15 ± 0.01	10.6 ± 0.5
silica gel, 25 Å	6.3×10^{-7}	0.15 ± 0.01	10.6 ± 0.4
silica gel, 25 Å	1.2×10^{-6}	0.18 ± 0.01	10.6 ± 0.4
silica gel, 25 Å, nitrogen purged	1.3×10^{-7}		26.0 ± 0.9
silica gel, 60 Å	2.5×10^{-7}	0.15 ± 0.03	7.1 ± 0.8
silica gel, 150 Å	2.5×10^{-7}	0.07 ± 0.02	8.5 ± 0.9

[a] The errors in Φ_f are the standard deviations of at least three measurements with different samples; the errors in lifetime are the errors of the least-squares fitting of the decay curve.

With an increase in sample loading, the diffuse reflectance spectra of adsorbed BeP showed band broadening and negative deviations from the Kubelka−Munk theory.[32] A bathochromic shift and band broadening were also observed in the emission spectra. These changes were attributed to the formation of microcrystals on the surface at loadings higher than 10^{-6} mol/g.

Fluorescence yields and lifetimes were measured in solution and on adsorbed samples (Table 1). The Φ_f of BeP in acetonitrile under a nitrogen atmosphere was determined to be 0.08 ± 0.01. Similar values were obtained for BeP adsorbed on silica of 150 Å average pore diameter. These yields were much smaller than the 0.15 yield determined for BeP adsorbed on silica of 25 and 60 Å average pore diameter. The smaller Φ_f for BeP adsorbed on silica of larger pores was interpreted in terms of the higher

mobility experienced by BeP in these media in comparison to surfaces of smaller pore size. On the latter, the density of active sites is larger,[14] and the BeP molecules were expected to be more strongly adsorbed, thus exhibiting a lower mobility and also a decrease in the fraction of molecules decaying through nonradiative processes. The surface coverage by BeP affected the fluorescence quantum yield, since an increase in Φ_f was observed at higher loadings. Ruetten and Thomas also reported an increase in the Φ_f at high loadings for pyrene adsorbed on silica gel[14] and suggested this was due to weaker interactions of the pyrene molecules with the surface as the loading increased. They proposed the formation of charge-transfer (CT) complexes between the adsorbed pyrene and active sites on the surface. These CT sites present lower fluorescence quantum yields, a weak absorption band at 350 nm, and a short-lived emission that was red-shifted compared to the normal pyrene emission. At low surface loading, PAHs are preferentially adsorbed on these CT sites, and therefore exhibit lower emission efficiency. As the loading increases, the CT sites saturate and the additional PAH molecules are adsorbed on other adsorption sites that do not form CT complexes. Pyrene adsorbed on these other sites presents higher emission intensities, resulting in greater fluorescence quantum yields. The presence of CT complexes between adsorbed BeP and active sites on the surface could explain the increase of the Φ_f of BeP at high loadings. However, we do not have evidence of the formation of CT complexes of BeP adsorbed on silica gel.

The fluorescence lifetimes (τ) of BeP adsorbed on nonactivated silica gel in air were in the order of tens of nanoseconds (Table 1). These values are similar to that of BeP in solution, where τ was 15 ns. Oxygen quenched the excited singlet state, resulting in a 60% decrease in fluorescence lifetime. At the smaller pore size, the fluorescence lifetime was longer than that for BeP adsorbed on silica of 60 and 150 Å. This could be due to a lower quenching rate of the BeP singlet state by oxygen on the surface of smaller average pore diameter. When adsorbed on this surface, the BeP molecules are probably adsorbed mostly into the pores and therefore are less exposed to collisions with O_2 from the gas phase. Others have shown that fluorescence quenching is mainly dynamical for PAHs adsorbed on silica at room temperature.[12,14] No significant differences in τ were observed in samples of different loadings.

Time-Resolved Absorption. The time-resolved absorption spectra of laser-irradiated BeP in acetonitrile and methanol solutions presented a strong band with maximum at 435 nm, as depicted in Figure 2. The intensity of this band increased in the presence of electron scavengers such as O_2 and N_2O, suggesting that it corresponds to the absorption of the radical cation of BeP. In hexane solutions, this band did not appear because in this nonpolar solvent the radical ion and the electron are not solvated and thus are not stabilized enough to allow for charge separation.[33] The radical cation of BeP can be generated chemically by oxidation of the BeP molecule with concentrated sulfuric acid.[34] When an aliquot of a solution of BeP in hexane was added to concentrated sulfuric acid, an absorption band with a maximum at 430 nm appeared in the steady-state UV−vis spectrum (Figure 3). This band was similar in shape and spectral position to the band observed in the transient spectra of BeP in polar solvents under an oxygen atmosphere. This provided additional support for the assignment of the absorption band at 435 nm to the radical cation of BeP.

In addition to the radical band, two bands at 350 and 560 nm were observed in the transient spectra of BeP's solutions under N_2 atmosphere. These broad bands disappeared in the presence of oxygen and were assigned to a triplet−triplet absorption by comparing these with data reported in the literature.[35] The photophysical properties of the triplet of BeP in polar and nonpolar solvents measured in our laboratory are summarized in Table 2. The absorption coefficients (ϵ_T), as determined by the energy-transfer method,[21] were in good agreement with the values reported by Carmichael and Hug[23] for the BeP triplet in benzene. The results suggested that ϵ_T is independent of the solvent properties. The triplet quantum yields (Φ_T) were much higher in nonpolar than in polar solvents. This was attributable to a competition in polar solvents between triplet formation and photoionization to form the radical cation.

In the formation of the radical species, the transient absorptions of the triplet and the radical of BeP appeared during the laser pulse. Moreover, the decay of the triplet−triplet absorption did not affect the decay kinetics of the radical, implying that the triplet decay did not lead to the formation of the BeP radical

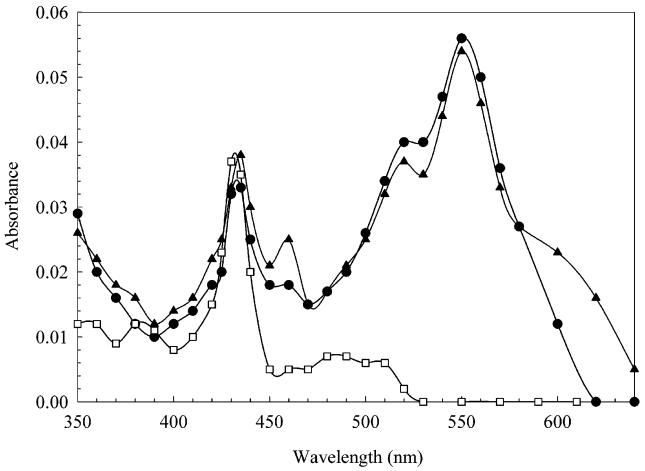

Figure 2. Transient spectra of BeP, 1×10^{-5} M, in acetonitrile under different atmospheres: O_2 (□), N_2 (●), and N_2O (▲), at a laser energy of 8 mJ and recorded 5×10^{-5} s after the laser pulse.

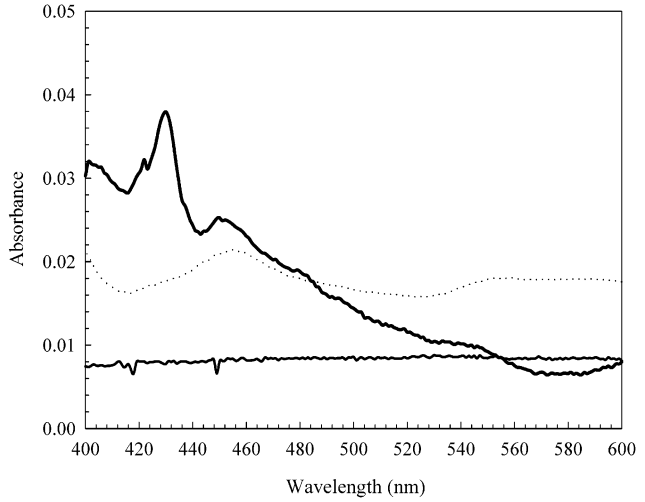

Figure 3. Absorption spectra of BeP in sulfuric acid (thick solid line) and in hexane (thin solid line). The band at 430 nm in the spectrum of BeP dissolved in sulfuric acid was assigned to the radical cation of BeP. The dotted line corresponds to the absorption spectrum of sulfuric acid without BeP added.

TABLE 2: Photophysical Properties of BeP's Triplet in Solution

solvent	ϵ_T (M^{-1} cm^{-1})	Φ_T	τ (μs)
acetonitrile	16 443 ± 1685	0.34 ± 0.05	52.1
hexane	17 716 ± 1733	0.68 ± 0.08	53.4

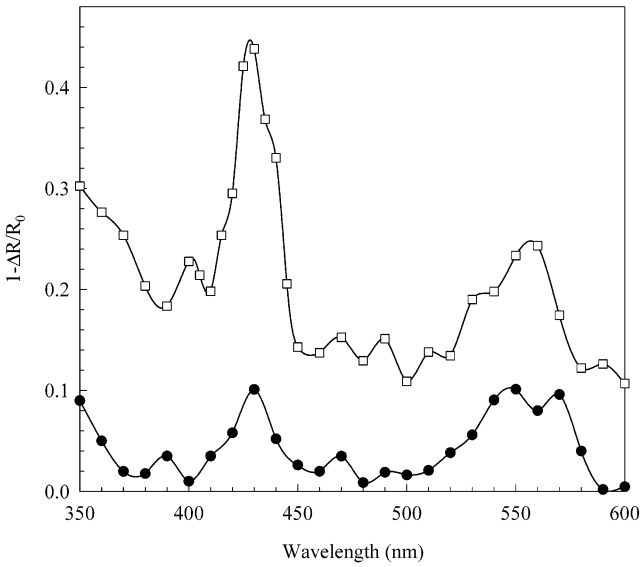

Figure 4. Transient diffuse reflectance spectra of BeP adsorbed on silica gel (□) and on alumina (●) under N_2 atmosphere. The laser energy was 20 mJ.

cation. Also, in O_2-saturated solutions, where the triplet-state absorption was quenched, no significant effects on the radical cation initial yield were observed. Thus, it was concluded that the radical cation of BeP originates from an excited singlet state rather than from a triplet state.

Time-resolved diffuse reflectance laser flash spectra of BeP were obtained under air, N_2, and O_2 atmospheres, at different loading concentrations, in the presence of coadsorbed water, on silica gels of different average pore size and on alumina. Laser-irradiated samples of BeP adsorbed on silica gel under an air atmosphere showed an absorption band at 430 nm (Figure 4), similar to that assigned to the BeP radical cation in polar solvents. The intensity of the band at 430 nm increased in the presence of oxygen, indicating that O_2 either promoted electron-transfer reactions or prevented ion−electron recombination on the silica gel surface. The decay of the radical cations presented an initial fast fall, followed by a slow decay. These nonexponential decay curves are typical for the decay of PAH radical cations adsorbed on silica and alumina surfaces. This behavior has been ascribed to the existence of a distribution of PAH cations produced at different active sites, decaying as a result of geminate recombination with the electron.[11] The initial intensity of the 430 nm band increased with decreasing pore size (Figure 5). The surface pore size also affected the radical decay rate, resulting in a faster decay in samples of 150 Å pore size diameter. Studying a different family of adsorbed compounds, Xiang and Kevan[36] reported on the effect of pore size of the silica on the photooxidation of phenothiazine derivatives. They found that, in silica gels of small pores, the methylphenothiazine radical cation had a larger photoyield and was more stable than in silica of larger pore diameter. A greater mobility of the adsorbed molecules on silica of larger pores can be responsible for the lower stability and yield of BeP and phenothiazine radical cations.

Monophotonic ionization was observed for BeP adsorbed on the surface as well as in solution. This was demonstrated from a linear relationship with zero intercept of the absorbance of the radical cation band at 430 nm as a function of the laser excitation energy (Figure 6). These measurements were made under an oxygen atmosphere to minimize the possible contribution of the triplet−triplet absorbance to the radical signal. A logarithmic plot of the reflectance function [$F(R) = 1 - \Delta R/R_0$] versus the laser energy is shown in the inset of Figure 6. The slope of this plot is 1.09, providing further evidence that the photoionization is a single-photon process. At laser energies higher than 15 mJ, the plot of absorbance vs energy reached a nonlinear region due to a partial saturation phenomenon. This is due to both the large amount of light absorbed by BeP and the substantial ground-state depletion at high laser fluencies. At these energies, all the exposed molecules that are capable of yielding a radical had reacted; thus, a further increase of the excitation energy did not result in the formation of additional radical cations. The ionization energy of BeP in the gas phase is 7.62 eV, whereas the energy of a photon at 266 nm is only 4.66 eV.[19] It is evident that the energy of one photon at this wavelength is not large enough to eject an electron from the BeP molecule. Therefore, the photoionization of PAHs might occur through the following two processes: through a triplet state as intermediate (two-photon process), or through the formation of a charge-transfer complex (single-photon process). The ionization of BeP in the surface was clearly monophotonic; thus, it is proposed that the later mechanism was taking place. It has been postulated that the first excited singlet state of PAHs can form a charge-transfer complex either with the silanol groups of the silica or with oxygen molecules physisorbed on the surface.[33] Turro et al.[37] claimed that peroxide defect sites present on the silica gel are principally responsible for the charge-transfer complexes' formation with aromatic hydrocarbons.

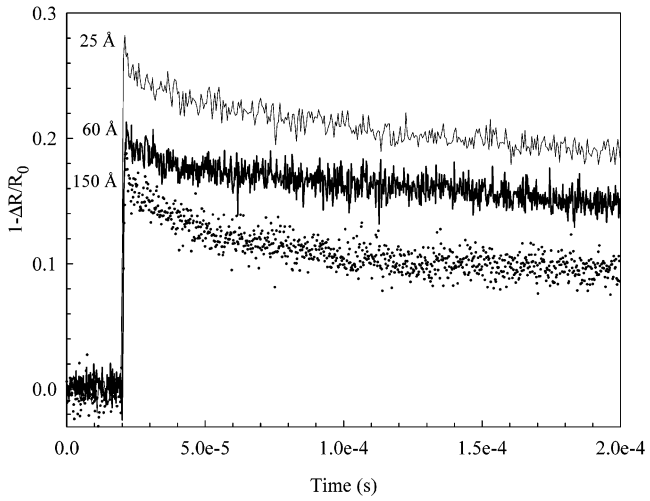

Figure 5. Decay kinetics of the BeP radical cation (430 nm) adsorbed on silica gel of different pore sizes under an air atmosphere. The surface loading was 3×10^{-7} mol/g, and the laser energy was 15 mJ.

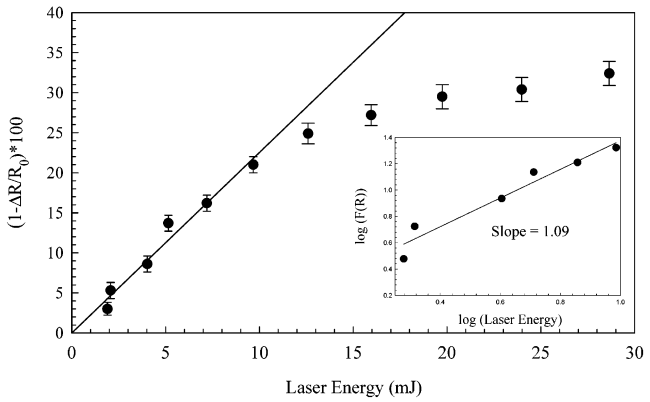

Figure 6. Photoionization of BeP adsorbed on silica gel under an oxygen atmosphere. The surface loading was 3×10^{-7} mol/g, and the excitation wavelength 266 nm. The inset shows the logarithmic plot of the reflectance function [$F(R) = 1 - \Delta R/R_0$] versus the laser energy.

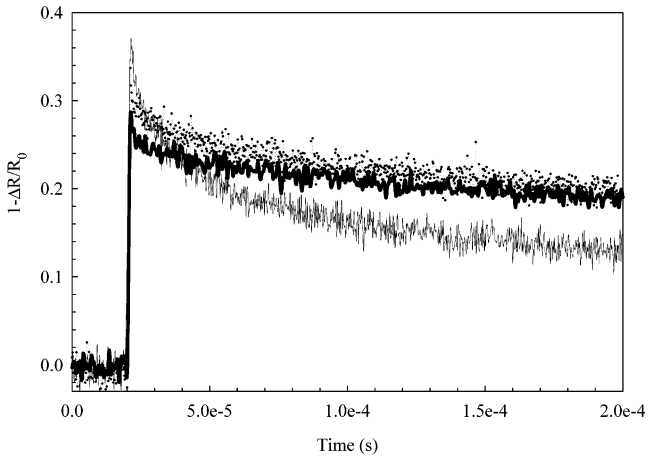

Figure 7. Radical decay (430 nm) of BeP adsorbed on silica of 25 Å pore size at different surface loadings: thin solid line, 1×10^{-6}; dotted line, 8×10^{-7}; and thick solid line, 3×10^{-7} mol/g under an air atmosphere, laser energy of 15 mJ.

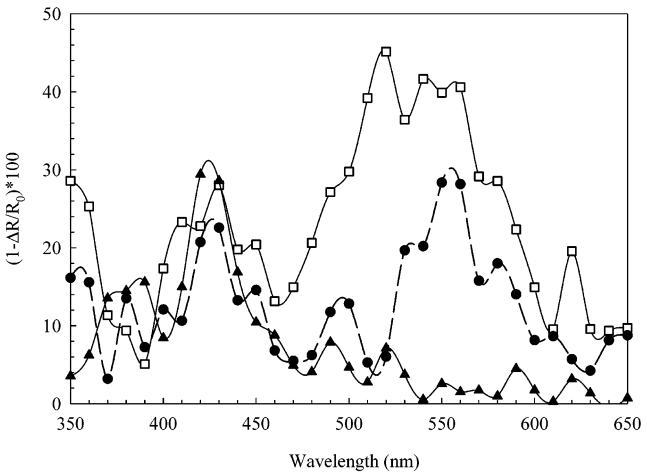

Figure 8. Transient diffuse reflectance spectra of BeP adsorbed on dry silica under N_2 (□), O_2 (▲), and N_2O (●) atmospheres. The surface loading was 1×10^{-6} mol/g, and the laser energy was 15 mJ.

The shape of the transient diffuse reflectance spectra of BeP adsorbed on silica of 25 Å pore size did not change with increasing surface loading. However, as depicted in Figure 7, the decay kinetics of the BeP radical cation was dramatically affected by the loading on the surface. At loadings of 1×10^{-6} mol/g or higher, an initial fast component was observed on the radical decay curve. The radical decay of PAHs adsorbed on inorganic oxides at low surface loadings occurs mainly through ion−electron recombination,[38] and the rate of these processes is strongly dependent on the surface nature and on the active sites' distribution.[39] At high loadings, an additional radical decay channel could arise from the reaction of two close PAH radicals to form dimers. At loadings of 1×10^{-6} mol/g and higher, the formation of aggregates of BeP adsorbed on silica was noted, demonstrated by a red shift and broadening of the fluorescence emission spectra.[40] The formation of dimers was not observed, even when the adsorbed BeP was irradiated at these high loadings. Therefore, the initial fast decay of the BeP radical at high loadings did not result from bimolecular reactions. It has been previously shown that, at high loading, electrons can combine with radical cations other than their parent as the cation−cation separation approaches the cation−electron separation.[39] At these high loadings, bulk electron diffusion competes efficiently with the geminate recombination observed at low loadings. The fast initial decay could also be accounted for in terms that an increase in the BeP loading results in its adsorption in more open or flat regions of the surface, and this population is more exposed to O_2 from the gas phase, thus resulting in an increase in the reaction of the radical with oxygen.

Bands attributable to triplet formation were observed at 350 and 560 nm (Figure 4) in samples of BeP purged with nitrogen and adsorbed on silica of 25 and 60 Å pore size, but not for BeP adsorbed on silica gel with an average pore size of 150 Å. Due to greater mobility, the BeP molecules on silica with larger pores were more exposed to any residual oxygen and to dynamical quenching reactions, resulting in a higher probability of triplet decay. Nonetheless, the photodegradation rate of BeP on this surface (data not shown) was similar to that of the compound adsorbed on silica of smaller pore diameters,[40] suggesting that the triplet did not play a fundamental role in the photodegradation mechanism. Samples of BeP adsorbed on alumina also showed the radical and triplet bands, but these were 5 times less intense than those observed in silica (Figure 4). This finding is in accordance with the low photodegradation rates observed for BeP adsorbed on alumina. The decay rate of the BeP radical adsorbed on alumina was more than twice as fast as that on silica at a similar loading. Thus, the low photoreaction of BeP adsorbed on alumina could arise from a lower yield of its reactive radical cation on this surface or from weak stabilization of the radical and the electron, leading to a fast recombination of these species.

The radical and the triplet absorption bands were observed in samples of BeP adsorbed on silica with coadsorbed water. The intensity of these bands was lower than the intensity of samples without water added at the same loading. The decay rate of the BeP radical was also affected, being faster in the absence of water. Transient studies of dry samples were performed to evaluate the effect of the physisorbed water on the intermediate species in the photodegradation of BeP. Broadening of the radical cation absorption band at 430 nm and an intense band at 520 nm were observed in the transient diffuse reflectance of BeP adsorbed on dry silica of 25 Å pore size (Figure 8). These bands disappeared in the presence of electron scavengers such as O_2 and N_2O, suggesting contributions from absorptions of a radical anion of BeP. Since the absorption spectrum for this species has not been reported in the literature, this band assignment could not be confirmed. However, the presence of pyrene radical anion has been proposed during the photolysis of this PAH adsorbed on zeolites and in a glassy matrix.[41] Because the ground-state absorption spectra of pyrene and benzo[*e*]pyrene and their corresponding radical cations are similar, the absorption spectra of their radical anions were expected to follow a similar trend. The radical anion of pyrene presents a maximum absorption band at 490 nm[41] that is shifted to the blue by only 30 nm with respect to the signal observed for BeP on dry silica. This observation lends additional support to the assignment of the 520 nm absorption band to the BeP radical anion.

Electron Spin Resonance Studies. The presence of the radical cation of BeP in irradiated adsorbed samples was confirmed by ESR studies. The ESR spectra of irradiated BeP samples adsorbed on silica and on alumina at 77 K were broad, partially resolved, and asymmetric. The signal was centered at 3400 G with a *g* value of 2.0055 that corresponds to the radical cation (Figure 9). Un-irradiated samples adsorbed on silica did not present a signal. Although the shape of the spectra did not change, the intensity of the BeP radical signal increased with irradiation time. After warming of the irradiated sample at 77 K to room temperature and cooling back to 77 K, the ESR signal was still observed, but at a lower intensity. In alumina, the very

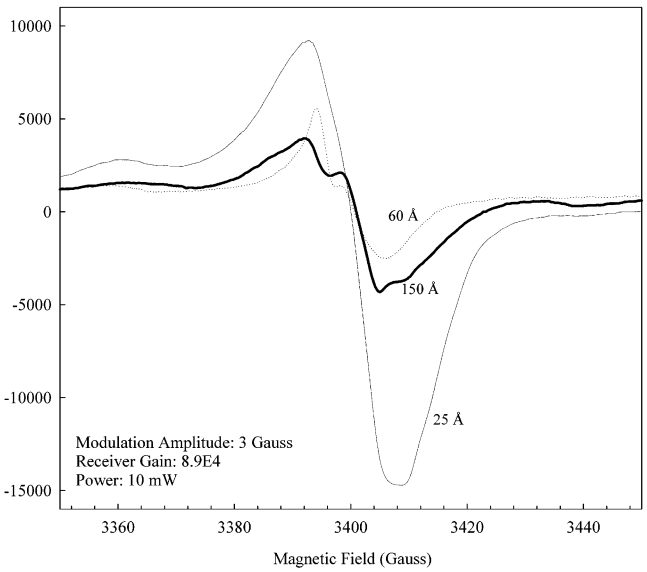

Figure 9. ESR spectra of BeP adsorbed on silica gel of different pore sizes at 77 K. Surface loading, 3×10^{-7} mol/g; irradiation time, 15 min.

weak ESR signal indicated that the radical yield of BeP was low, in accordance with the low photoreactivity observed for BeP on this surface. At a loading of 3×10^{-7} mol/g, the calculated *g* values for the BeP radical cations were in the range of 2.0055−2.0060 for the different surfaces, very close to that of the free electron (2.00232), as is the case for most organic radicals. On silica of 25 Å pore size at a higher loading (10^{-6} mol/g), or in surfaces with water added, small changes in g ($\Delta g = 0.0012$) were observed, suggesting different orientations of the radical adsorbed under these different conditions. Although some hyperfine structure was observed in the ESR signal (Figure 9) in samples adsorbed on silica of larger pore sizes (60 and 150 Å), fine structure was not observed for BeP adsorbed on silica of 25 Å pore size, due to the loss of mobility of the radical adsorbed on that substrate. In general, the ESR spectral resolution and line width of adsorbed radicals depend on their mobility on the surface. Radicals of organic molecules adsorbed on silica and alumina present broad signals without hyperfine structure, due to the immobilization of the adsorbed radicals.[28] Thus, the observed fine structure implied that the BeP radical experiences some mobility on the surfaces of larger pores, in contrast to restricted movement on silica gel of 25 Å. Kevan et al. reported differences in the mobility and radical yield of *N*-alkylphenothiazines as a function of the pore size of the adsorbent.[42] Using silica-based molecular sieves of controlled pore size as adsorbents, they observed a greater mobility and a smaller radical photoyield for large cavities (approximately 100 Å pore size), and lower mobility and radical yield for surfaces with pore sizes of approximately 25 Å.

A broad, weak signal was also observed in the low field of the ESR spectra of photolyzed samples of BeP adsorbed on silica with a *g* value of 2.0280, and a different saturation behavior relative to the central line. This signal was assigned to the peroxy radical ($O_2^{\bullet -}$) because its shape and *g* factor were consistent with those reported for $O_2^{\bullet -}$ in other studies of irradiated PAHs on silica and alumina.[43] The formation of $O_2^{\bullet -}$ suggested that BeP could react with physically adsorbed O_2 on the surface by an electron-transfer reaction from the excited PAH to oxygen.

$$O_2 + \text{BeP*/SiOH} \rightarrow \text{BeP}^{\bullet +}\text{/SiOH} + O_2^{\bullet -}\text{/SiOH} \quad (2)$$

However, this is not the only mechanism for the formation of the BeP radical cation on the surface, because it was also observed in the laser diffuse reflectance studies performed in the absence of oxygen.

In the ESR experiments, the BeP samples were irradiated with a continuous arc lamp, and the photoionization of BeP was clearly observed. This lamp does not provide photon fluxes as large as required to induce biphotonic ionization. Additionally, our transient absorption results demonstrated that the formation of the radical cation of BeP originates from an excited singlet state and not from the triplet. These facts support the hypothesis that the ionization process of BeP adsorbed on the surface proceeds through a charge-transfer complex mechanism.

Photodegradation Mechanism. Photodegradation studies of BeP adsorbed on silica using methylene blue as a singlet oxygen sensitizer were performed to investigate the mechanism of formation of photoproducts. Samples of BeP on silica with co-adsorbed methylene blue, irradiated at wavelengths longer than 550 nm, did not reveal BeP decomposition, even after 40 h of irradiation. This suggested that the photodegradation of BeP on the surface occurs through participation of the BeP radical cation and not via reaction of BeP with singlet oxygen.

Some photoproducts of BeP adsorbed on silica gel were isolated and characterized. One of the main products was identified as 4,5-benzo[*e*]pyrenedione. It was characterized by absorption spectroscopy, fluorescence, and mass spectrometry. Its electrospray mass spectrum presents a molecular ion at 283.3 *m*/*z* that corresponds to the M + H ion. The identity of this dione was confirmed by co-injection with a standard solution of 4,5-benzo[*e*]pyrenedione. 4,5-Benzo[*e*]pyrenediol was also identified as a photoproduct. Its UV−visible spectrum is identical to that previously reported in the literature.[44] 1-Hydroxybenzo[*e*]pyrene was identified as a minor photoproduct by mass spectrometry (major peak at 267.3 *m*/*z* corresponding to the M − H ion) and by comparison of its absorption spectrum with that reported in the literature[45] (maximum absorption at 225 nm). Another minor product was identified as 3-hydroxybenzo[*e*]pyrene with absorption maxima at 387, 341, and 296 nm, and an electrospray mass spectrum presenting only one peak at 267.2 *m*/*z*. Its identity was confirmed by co-injection with a standard solution of 3-hydroxybenzo[*e*]pyrene. Another photoproduct that was isolated presented a 283.2 *m*/*z* peak on its mass spectrum and was tentatively assigned to a dione. The absorption spectrum of this dione presents several unresolved absorption maxima in the range of 250−550 nm. Only two diones of BeP are reported in the literature, 4,5-benzo[*e*]pyrenedione and its 9,10 isomer. The UV−vis spectrum of the dione isolated in our studies is very different from that of 9,10-benzo[*e*]pyrenedione,[46] but we could not establish the exact isomeric structure of this photoproduct.

Irradiation of solutions of BeP in hexane did not lead to the formation of the diones and hydroxy derivatives that were observed in polar solvents or when BeP was adsorbed on surfaces. In hexane, the radical cation was not observed; this implies that the radical cation was the intermediate species involved in the formation of these photoproducts. The irradiation of BeP adsorbed on dry silica did not produce any of the products observed during the photodegradation in nondried silica. However, the radical cation absorption band was observed in the transient spectra of the dry samples, implying that the water adsorbed on the surface plays a fundamental role in the formation of the photoproducts.

Conclusions

The intermediate species involved in the photolysis of BeP were identified and characterized in order to provide information

on BeP's photodegradation mechanism. Our results indicate that the photodegradation of BeP adsorbed on the surfaces and in polar solvents occurs through a radical-cation-mediated mechanism instead of via a reaction of the PAH with singlet oxygen. The presence of BeP's radical cation was established for samples of BeP adsorbed on silica gel and alumina, as well as in samples of BeP dissolved in polar solvents. However, this intermediate is not observed in solutions of BeP in hexane, suggesting that the photodegradation in nonpolar solvents occurred through a different pathway.

The radical cation of BeP originates from an excited singlet state by a single-photon process. The BeP radical can react with water to yield photoproducts such as diones, diols, and alcohols.[17] The excited triplet state of BeP was also detected as a transient species in adsorbed samples and in solution under a nitrogen atmosphere. However, it did not play a major role in the photodegradation mechanism. The photochemical processes involved in the photodegradation of BeP can be summarized by the following reactions:

$$\mathrm{BeP} + h\nu \rightarrow {}^1\mathrm{BeP}^* \quad (3)$$

$${}^1\mathrm{BeP}^* \rightarrow {}^3\mathrm{BeP} \quad (4)$$

$${}^1\mathrm{BeP}^* \rightarrow \mathrm{BeP} + h\nu' \quad (5)$$

$${}^1\mathrm{BeP}^*/\mathrm{surface} \rightarrow [\mathrm{CT\ complex}] \rightarrow \mathrm{BeP}^{\bullet+} + \mathrm{e}^- \quad (6)$$

$${}^1\mathrm{BeP}^* + \mathrm{O_2} \rightarrow \mathrm{BeP}^{\bullet+} + \mathrm{O_2}^{\bullet-} \quad (7)$$

$$\mathrm{BeP}^{\bullet+} + \mathrm{H_2O/O_2} \rightarrow \mathrm{photoproducts} \quad (8)$$

The surface's nature, pore size, and presence of coadsorbed water affected the yield of intermediates and kinetics but did not affect the photodegradation mechanism. A greater mobility of BeP adsorbed on surfaces with larger pores could account for the lower radical yield and the shorter $\mathrm{BeP}^{\bullet+}$ lifetimes observed on silica of 150 Å pore size. The formation of BeP radical cations, when adsorbed on alumina, through irradiation was much less efficient than on silica. Also, the $\mathrm{BeP}^{\bullet+}$ was less stable on alumina, which could explain the lower photodegradation rates reported for BeP on this surface.[39]

Benzo[*e*]pyrene is an ubiquitous pollutant, thermally stable and resistant to chemical degradation. Thus, photodegradation is one of the major pathways of natural removal of this contaminant from the environment. We have demonstrated that BeP adsorbed on silica or alumina and also in solution reacts photochemically to produce a radical cation. Further reactions of this radical with water and oxygen yield oxidized derivatives such as diones, diols, and alcohols. Aromatic radicals and diones are very reactive species, capable of producing extensive DNA damage. Therefore, the photochemical degradation of BeP in the atmosphere could be a process that increases the toxicity of the particulate matter instead of a method of natural remediation.

Acknowledgment. We acknowledge financial support from DOE-EPSCoR (DE-FG029ER755764) and NSF-EPSCoR. We also acknowledge Dr. Alegría at UPR-Humacao for the use of the ESR facilities.

References and Notes

(1) Leiter, J.; Shimkin, M. B.; Shear, M. J. *J. Natl. Cancer Inst.* **1942**, *3*, 155.

(2) U. S. National Academy of Sciences. *Polycyclic Aromatic Hydrocarbons: Evaluation of Sources and Effects*; Committee on pyrene selected analogues, Board on toxicological and environmental health hazards, Commission on Life Sciences & National Research Council, National Academy Press: Washington DC, 1983; Appendix B.

(3) Blumer, M. *Sci. Am.* **1976**, *234*, 25.

(4) O'Connor, T. P. *Coastal Environmental Quality in the United States*; NOAA Coastal Monitoring Branch: Rockville, MD, 1990.

(5) Wood, A. W.; Levin, W.; Thakker, D. R.; Yagi, H.; Chang, R. L.; Ryan, D. E.; Thomas, P. E.; Dansette, P. M.; Whittaker, N.; Turujman, S.; Lehr, R. E.; Kumar, S.; Jerina, D. M.; Conney, A. H. *J. Biol. Chem.* **1979**, *254*, 4408.

(6) (a) Rogan, E.; Roth, R.; Katomski, P.; Benderson, J. Cavalieri, E. *Chem. Biol. Interact.* **1978**, *22*, 35. (b) Rogan, E.; Hakan, A.; Cavalieri, E. *Chem. Biol. Interact.* **1983**, *47*, 111. (c) Sims, P.; Grover, P. L.; Swaisland, A.; Pal, K.; Hewer, A. *Nature* **1974**, *252*, 326. (d) Jerina, D. M.; Daly, J. W. *Science* **1974**, *185*, 573.

(7) Dabestani, R. *Inter-Am. Photochem. Soc. Newsl.* **1997**, *20*, 24.

(8) Ramamurthy, V.; Schanze, K. S. *Solid State and Surface Photochemistry*; Marcel Dekker: New York, 2000.

(9) Sigman, M. E.; Barbas, J. T.; Chevis, E. A.; Dabestani, R. *New J. Chem.* **1996**, *20*, 243.

(10) Dabestani, R.; Ellis, K. J.; Sigman, M. E. *J. Photochem. Photobiol. A* **1995**, *86*, 231.

(11) Pankasem, S.; Thomas, J. K. *J. Phys. Chem.* **1991**, *95*, 6990.

(12) Thomas, J. K. *Chem. Rev.* **1993**, *93*, 301.

(13) Bauer, R. K.; Borenstein, R.; De Mayo, P.; Okada, K.; Rafalska, M.; Ware, W. R.; Wu, K. C. *J. Am. Chem. Soc.* **1982**, *104*, 4635.

(14) Ruetten, S. A.; Thomas, J. K. *J. Phys. Chem. B* **1999**, *103*, 1278.

(15) Reyes, C.; Medina, M.; Crespo-Hernandez, C.; Cedeño, M.; Arce, R.; Rosario, O.; Steffenson, D. M.; Ivanov, I. N.; Sigman, M. E.; Dabestani, R. *Environ. Sci. Technol.* **2000**, *34*, 415.

(16) Baek, S. O.; Field, R. A.; Goldstone, M. E.; Kirk, P. W.; Lester, J. N.; Perry, R. *Water, Air, Soil Pollut.* **1991**, *60*, 279.

(17) Fioressi, S. Ph.D. Thesis, University of Puerto Rico, 2001.

(18) (a) Liu, Y. S.; Ware, W. R. *J. Phys. Chem.* **1993**, *97*, 5980. (b) Liu, Y. S.; Ware, W. R. *J. Phys. Chem.* **1993**, *97*, 5987. (c) Liu, Y. S.; Ware, W. R. *J. Phys. Chem.* **1993**, *97*, 5995.

(19) Dabestani, R.; Ivanov, I. N. *Photochem. Photobiol.* **1999**, *70*, 10.

(20) Oelkrug, D.; Honnen, W.; Wilkinson, F.; Willsher, C. J. *J. Chem. Soc., Faraday Trans. 2* **1987**, *83*, 2081.

(21) Bensasson, R.; Land, E. J. *Trans. Faraday Soc.* **1971**, *67*, 1904.

(22) Morgan, D. D.; Warshawsky, D.; Atkinson, T. *Photochem. Photobiol.* **1977**, *25*, 31.

(23) Carmichael, I.; Hug, G. *J. Phys. Chem. Ref. Data* **1985**, *15*, 1.

(24) Amand, B.; Bensasson, R. *Chem. Phys. Lett.* **1975**, *34* (1), 44.

(25) Bensasson, R.; Gramain, J. C. *J. Chem. Soc., Faraday Trans. 1* **1980**, *76*, 1801.

(26) Stevens, B.; Algar, B. E. *J. Phys. Chem.* **1968**, *72*, 3468.

(27) Horrocks, A. R.; Wilkinson, F. *Proc. R. Soc. London Ser. A* **1968**, *306*, 257.

(28) Wertz, J. E.; Bolton, J. R. *Electron Spin Resonance*; Chapman and Hall; New York, 1986.

(29) Ham, J. S. *J. Chem. Phys.* **1953**, *21*, 756.

(30) Kalyanasundaram, K.; Thomas, J. K. *J. Am. Chem. Soc.* **1977**, *99*, 2039.

(31) Pankasem, S.; Thomas, J. K. *J. Phys. Chem.* **1991**, *95*, 7385.

(32) Kubelka, P.; Munk, F. *Z. Tech. Phys.* **1931**, *12*, 539.

(33) Zimmermann, C.; Mohr, M.; Zipse, H.; Eichberger, R.; Schnabel, W. *J. Photochem. Photobiol. A* **1999**, *125*, 47.

(34) Rogan, E.; Roth, R.; Cavalieri, E. *Polynuclear Aromatic Hydrocarbons*; Bjorseth, A., Dennis, A. J., Eds.; Battelle Press: Columbus, OH, 1980; pp 259−266.

(35) (a) Pavlopoulos, T. G. *Ber. Bunsen-Ges. Phys. Chem.* **1970**, *74*, 989. (b) Slifkin, M. A.; Walmsley, R. H. *Photochem. Photobiol.* **1971**, *13*, 57.

(36) Xiang, B.; Kevan, L. *Langmuir* **1994**, *10*, 2688.

(37) Leheny, A. R.; Turro, N. J.; Drake, J. M. *J. Phys. Chem.* **1992**, *96*, 8498.

(38) Beck, G.; Thomas, J. K. *Chem. Phys. Lett.* **1983**, *94*, 553.

(39) Oelkrug, D.; Reich, S.; Wilkinson, F.; Leicester, P. A. *J. Phys. Chem.* **1991**, *95*, 269.

(40) Fioressi, S.; Arce, R. *Polycycl. Arom. Compd.* **1999**, *14*−*15*, 285.

(41) (a) Liu, X.; Mao, Y.; Ruetten, S. A.; Thomas, J. K. *Solar Energy Mater. Solar Cells* **1995**, *38*, 199. (b) Shida, T.; Iwata, S. *J. Am. Chem. Soc.* **1973**, *95*, 3473.

(42) Krishna, R. M.; Prakash, A. M.; Kevan, L. *J. Phys. Chem. B* **2000**, *104*, 1796.

(43) (a) Barbas, J. T.; Sigman, M. E.; Buchanan, A. C., III; Chevis, E. A. *Photochem. Photobiol.* **1993**, *58*, 155. (b) Mao, Y.; Thomas, J. K. *Chem. Phys. Lett.* **1994**, *226*, 127.

(44) Lehr, R. E.; Taylor, C. W.; Kumar, S. *J. Org. Chem.* **1978**, *43*, 3462.

(45) Lee, H.; Shyamasundar, N.; Harvey, R. G. *J. Org. Chem.* **1981**, *46*, 2889.

(46) Platt, K. L.; Oesch, F. *Tetrahedron Lett.* **1982**, *23*, 163.